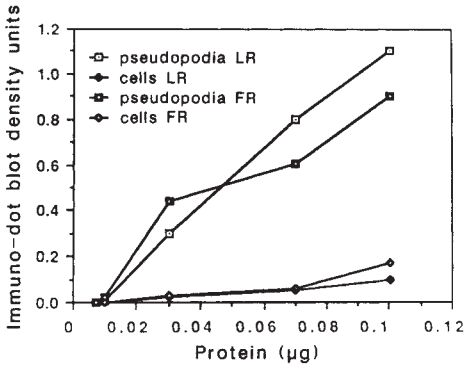

Fig. 3 Augmentation of laminin receptor (LR) and fibronectin receptor (FR) (RGD recognition) antigen on isolated pseudopodia. Receptor antigen content of detergent extracted isolated pseudopodial plasma membranes (pseudopodia) compared to whole cell plasma mebranes (cell). Quantitative immuno-dot blotting was performed as described[16]. Each data point represents the mean of three determinations using matched 1/500 antibody dilutions and the indicated amount of extracted pseudopodia or cell protein. Anti-fibronectin receptor antibodies described previously[8,9] were supplied by Dr W. T. Chen of Georgetown University, Washington, DC. Anti-laminin receptor monoclonal antibodies and plasma membrane extractions were prepared and characterized as described previously[15].

Boyden chamber were attached to the surface of polycarbonate filters having a pore size which prevented whole cell traversal but allowed the protrusion of pesudopodia (Fig. 1*c–e*). The induced pseudopodia were collected from the opposite face of the filter by adherence to glass (Fig. 2) or by mechanical scraping. This method demonstrated that pseudopodia protrusion was induced by AMF in a time- and dose-dependent manner (Fig. 2) and began ~30 min before whole cell translocation. Preincubation of AMF with anti-AMF antibodies inhibited the induction of pseudopodia in parallel with inhibition of motility (Fig. 2*d*).

Checkerboard analysis (Fig. 2*c*) was used to establish whether AMF induced random or directed pseudopodia formation. When AMF was introduced into either or both chambers, pseudopodia protrusion was extensive, so we conclude that AMF stimulates random pseudopodia formation and does not require a gradient of AMF to orient the pseudopodia. This agrees with the finding that AMF also stimulates random motility to a much greater degree than directed motility[4].

Ultrastructural studies of pseudopodia induced by AMF showed that they frequently contained bundles of actin cables along the long axis of the pseudopod (Fig. 1). The actin cables terminated at the inner membrane zone of the leading edge of the pseudopodia. It has been proposed that cytoplasmic actin bundles bind indirectly to the cytoplasmic domain of transmembrane extracellular matrix (ECM) receptors[8–10]. Furthermore, ultrastructural studies of tumour cells migrating through the rat mesentery have suggested that the tips of cell pseudopodia form receptor-mediated contacts with the ECM[3]. AMF-stimulated pseudopodia are an ideal system to study whether or not ECM receptors pre-exist on the pseudopodia or are induced only when the pseudopod is adherent to the ECM component. It has been suggested that ECM receptors are randomly distributed on the surface of the cell and that the anchorage of the receptor to the extracellular ligand regulates the distribution of the receptor. But in the migrating tumour cell, which involves reversible attachment as part of the locomotory response, the distribution of ECM receptors is not random. When AMF stimulates the formation of pseudopodia before the locomotion cascade, an asymmetric distribution of receptors occurs, with a higher concentration in the pseudopods than in the membranes of unstimulated cells. We find that AMF-induced isolated pseudopia contain 20 times more laminin and fibronectin Arg-Gly-Asp (RGD) recognition receptors (Fig. 3) than the average number found in the plasma membrane of unstimulated cells. AMF can stimulate pseudopodia formation and migration on a variety of adhesive substrata, including uncoated polycarbonate filters or polycarbonate filters coated with fibronectin, laminin, type IV collagen, or type I collagen (Table 1). As pseudopodia can be induced by AMF in the absence of a laminin- or fibronectin-coated substratum, the increase in the number of receptors on the pseudopodia must precede their interaction with extrinsic laminin and fibronectin.

Pseudopodia induction by soluble factors has been previously limited to polymorphonuclear leukocytes migrating in a gradient or uniform concentrations of a chemoattractant[11]. This study demonstrates that uniform concentrations of a cytokine are sufficient to induce psuedopodia formation and subsequent translocation of the cell. We conclude that pseudopodia formation is an integral component of cytokine-regulated tumour cell locomotion. Pseudopodia regulation can occur in a manner independent of the adhesion mechanism, although some type of adhesion is required for cell traction[12,13]. Autonomous random cell motility could begin with the induction of exploratory pseudopodia before cell translocation. ECM receptors concentrated on the surface of the pseudopodia might sense the distribution of ECM components in the immediate cellular environment and in turn help determine the vectorial direction of locomotion.

Received 9 July; accepted 6 August 1987.

1. Couchman, J. R., Lenn, M. *Eur. J. Cell Biol.* **36**, 182-194 (1985).
2. Mohler, J. L., Partin, A. W., Isaacs, W. B. & Coffey, D. S. *J. Urol.* **137**, 544-547 (1987).
3. Muller, G. W., Haemmerli, G. & Strauli, P. *Cell Biol. int. Rep.* **9**, 447-461 (1985).
4. Liotta, L. A. *et al. Proc. natn. Acad. Sci. U.S.A.* **83**, 3302-3306 (1986).
5. Stoker, M., Gherardi, E., Perryman, M. & Gray, J. *Nature* **327**, 239-242 (1987).
6. Atnip, K. D., Haney, L., Nicolson, G. L. & Dabbous, M. K. *Biochem. biophys. Res. Commun.* **146**, 996-1002 (1987).
7. Stracke, M. L., Guirgius, R., Liotta, L. A. & Schiffmann, E. *Biochem. biophys. Res. Commun.* **146**, 339-345 (1987).
8. Chen, W. T., Wang, J., Hasegawa, T., Yamada, S. S. & Yamada, K. M. *J. Cell Biol.* **103**, 1649-1661 (1986).
9. Chen, W. T., Chen, J. M. & Mueller, S. C. *J. Cell Biol.* **103**, 1073-1090 (1986).
10. Ruoslahti, E. & Pierschbacher, M. D. *Cell* **44**, 517-518 (1986).
11. Gallin, J. I., Gallin, E. K., Malech, H. L. & Cramer, E. B. in *Leukocyte Chemotaxis* (eds Gallin, J. I. & Quie, P. G.) 123-141 (Raven, New York, 1978).
12. Pryzwansky, K. B., Schliwa, M. & Porter, K. R. *Eur. J. Cell Biol.* **30**, 544-547 (1983).
13. Trinkaus, J. P. *J. Neurosci. Res.* **13**, 1-19 (1985).
14. Carter, S. B. *Nature* **208**, 1183-1187 (1965).
15. Wewer, U. M. *et al. Proc. natn. Acad. Sci. U.S.A.* **83**, 7137-7141 (1986).
16. Towbin, H. & Gordon, J. *J. immun. Meth.* **72**, 313-340 (1984).

Importance of DNA stiffness in protein–DNA binding specificity

M. E. Hogan* & R. H. Austin†

* Department of Molecular Biology and † Department of Physics, Princeton University, Princeton, New Jersey 08544, USA

From the first high-resolution structure of a repressor bound specifically to its DNA recognition sequence[1] it has been shown that the phage 434 repressor protein binds as a dimer to the helix. Tight, local interactions are made at the ends of the binding site, causing the central four base pairs (bp) to become bent and overtwisted. The centre of the operator is not in contact with protein but repressor binding affinity can be reduced at least 50-fold in response to a sequence change there[2]. This observation might be explained should the structure of the intervening DNA segment vary with its sequence, or if DNA at the centre of the operator resists the torsional and bending deformation necessary for complex formation in a sequence dependent fashion. We have considered the second hypothesis by demonstrating that DNA stiffness

is sequence dependent. A method is formulated for calculating the stiffness of any particular DNA sequence, and we show that this predicted relationship between sequence and stiffness can explain the repressor binding data in a quantitative manner. We propose that the elastic properties of DNA may be of general importance to an understanding of protein–DNA binding specificity.

The fact that DNA behaves as a stiff elastic rod has been recognized since Peterlin's early analysis of light scattering data[3]. This rigidity is expressed as the persistence length P of the molecule, which is related to the Young's modulus, E (ref. 4):

$$P = EI/kT \quad (1)$$

where I is the surface moment of inertia for a right cylinder, k is Boltzmann's constant and T is the absolute temperature; E is related to the stress which develops when the long axis of a rod is strained. The intrinsic shear modulus, G, relates the restoring stress when a lateral or torsional strain is applied to the material. The Young's and shear moduli are related by Poisson's ratio μ, which is also intrinsic:

$$G = E/2(1+\mu) \quad (2)$$

where μ is close to 0.5 for polymeric materials[5,6].

Recently, it has been found that E and G are not constant for DNA, but are a function of bp composition[7–10] which is not surprising as the stacking and the hydrogen bonding stabilizing DNA are strongest for G·C bps. The available experiments do not measure the intrinsic moduli directly, but instead the extrinsic bending constant B and the torsional constant C, given by;

$$C = IG/L \quad (3)$$

and

$$B = EIL \quad (4)$$

where L is the length of the molecule under strain and I is the area moment of inertia.

In Table 1 we present measured values for the Young's modulus of DNA as a function of base composition. Although the modulus E is the fundamental parameter, physical techniques measure EI. To extract E from those data, we have calculated I, using the crystallographic radius for B-DNA (11 Å), although it will be shown that the significant conclusions to be drawn from these analyses are not dependent on the value chosen. It is clear that the available data are not comprehensive, and the theories used to calculate EI from the data not perfect, especially in analysis of anisotropy and quenching data. Consequently, when the individual methods are applied to similar random sequence DNA samples, calculated values for E can vary by as much as a factor of three. Nevertheless, there is a good qualitative agreement among the various methods which we have emphasized by normalizing the outcome of each, so that for a random sequence DNA (45% G+C) the Young's modulus is adjusted to a traditional value (1.1×10^9 dyn cm^{-2}), corresponding to a persistence length of 175 bps at 300 K. Although this normalization is not strictly valid, the arguments presented below show this first order correction provides a useful insight into the properties of DNA.

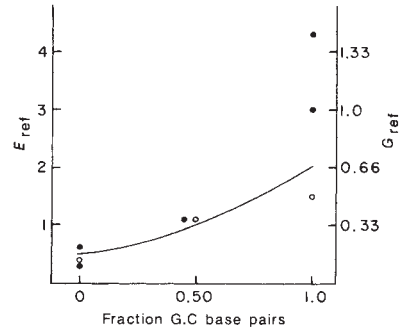

Fig. 1 Summary of the relation between stiffness and DNA sequence. The normalized Young's moduli E catalogued in Table 1 have been plotted against the mole fraction of G·C bps in the helix being studied. The corresponding shear moduli (G_{ref}) have been calculated from the Young's modulus, as described in the text. Solid line, compositional dependence predicted by equations (9) and (10) for random DNA sequences, using the consensus stiffness parameters in Table 2. ●, Measurements on random sequences or non-alternating synthetic helices, such as poly(dA).poly(dT); ○, measurements on DNA sequences with a simple alternating sequence, such as poly (dA-dT)·poly(dA-dT) or poly (dG-dC)·poly(dG-dC).

The shear modulus of DNA, G, is also presented in Table I, calculated from the Young's modulus using equation (2) and assuming that μ is 0.5, which has previously given close agreement with G as measured for DNA[7]. The relation does not hold for the homopolymer poly(dA)·poly(dT) (ref. 7), but this discrepancy could result from the atypical B-helix structure assumed by poly(A) sequences[11]. Because of this ambiguity, and because the Young's modulus of DNA has been measured by several methods whereas the shear modulus has not, our opinion is that, at present, the sequence dependence of DNA stiffness is best evaluated from calculations using the Young's modulus (as measured by light scattering, pulsed birefringence, triplet anisotropy decay and triplet quenching).

A conservative interpretation of the available data suggests that, at the extremes of base composition, E, and hence the bending and torsional stiffness of DNA, can vary by at least a factor of four (Fig. 1; Table 1).

Table 1 DNA flexibility measurements

Method / Sample	Triplet anisotropy $E(E_{ref})$	Birefringence $E(E_{ref})$	Light scatter $E(E_{ref})$	Triplet quenching $E(E_{ref})$	Consensus values E	Consensus values G
poly(dG)·poly(dC)	3.0 (2.4)			1.33 (4.3)	2	0.66
poly(dG-dC)·poly(dG-dC)			1.5 (1.5)		2	0.66
poly(dA-dC)·poly(dG-dT)	1.4 (1.1)				1	0.33
Random	1.4 (1.1)	1.1 (1.1)	1.1 (1.1)	0.34 (1.1)	1	0.33
poly(dA)·poly(dT)	0.8 (0.6)			0.10 (0.32)	0.5	0.167
poly(dA-dT)·poly(dA-dT)		0.36 (0.36)			0.5	0.167

These data are a compilation of data available in the literature. In each instance the Young's modulus E or shear modulus G has been presented in units of 10^9 dyne cm^{-2}. For each method which has been listed, a random sequence DNA was also measured. To compare the sequence dependence of those data more directly, we have normalized measured values E such that for each method, random sequence DNA is assigned the value 1.1×10^9. Those normalized moduli are presented in the parenthesis as E_{ref}. Triplet anisotropy[7] pulsed electric birefringence decay[8] light scattering[8] and triplet lifetime quenching[10] measurements are cited. For the birefringence and light scattering data, the original authors have calculated a persistence length for DNA. That value has been converted to a Young's modulus using equation (1) in the text and $I = 2.3 \times 10^{-28}$ cm^4. Consensus values for the Young's moduli E are an evaluation of the available literature and may be refined in the context of future experiments. Consensus values for G have been calculated using equation (2).

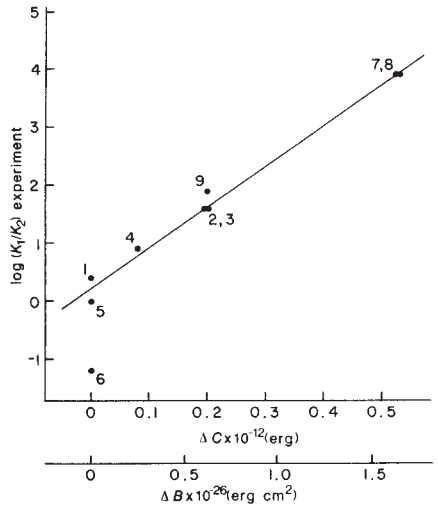

Fig. 2 Sequence dependence of 434 repressor binding: theory compared with experiment. The measured change in repressor binding affinity (from ref. 2) is compared to the change in DNA stiffness calculated from theory. See Table 2 for the numerical values. Experimental data are presented as log (K_1/K_2) plotted against ΔC or ΔB. Individual pairs (data against theory for each operator sequence) are identified by the numbering system in Table 2. Because C and B are proportional, their correlation with experiment has been presented together, by appropriate labelling of the abscissa. Solid line, linear least-squares analysis, assuming that the error in $\log(K_1/K_2)$ is ±0.2, as ascertained by the scatter of the binding data. A good linear correlation of that kind suggests that the measured binding constant change is determined by DNA stiffness effects.

Ethidium bromide fluorescence anisotropy experiments have surprisingly failed to detect sequence-dependent effects on the shear modulus[6,12]. The discrepancy between the ethidium bromide data and other physical measurements of DNA stiffness is a source of continuing controversy, but could be related to the fact that short-lived fluorescence decay measurements are most sensitive to high-frequency (local) motions of DNA, and for that reason are susceptible to changes in the DNA molecule which occur near the dye probe binding site. High-frequency DNA motions may be crucial to an understanding of its stability and function, but we will limit our present discussion of stiffness variation to results verified by several techniques.

To understand protein binding specificity in terms of DNA stiffness variation, it is first necessary to consider the work required to deform a helix. The mechanics of elastic media specifies that if a length L of DNA, with Young's modulus E and area moment of inertia I is strained by bending into an arc of radius S or twisting through an angle ϕ (in radians) the work done is;

$$U(\phi) = -IG\phi^2/2L = -C\phi^2/2 \quad (5)$$

and

$$U(S) = -EIL/2S^2 = -B/2S^2 \quad (6)$$

This linear elastic model may be too simple, because it overlooks the possibility that DNA bending and twisting are directional[13] and assumes that DNA can be modelled as a continuum rod. But, given that the same simplification is built into theories used to interpret the hydrodynamic and scattering data (see Table 1), the above equations are adequate approximations.

To complete our model, it is necessary to describe how the contribution of individual bps sums to produce a net bending constant B and torsional constant C. DNA flexibility as measured experimentally does not involve a disruption of bps but is a property of the duplex state, so sequence-dependent stiffness variation must be a function for the vertical (base-stacking) interaction between the bps. To a first approximation then, the stiffness of a DNA segment should vary as the frequency of nearest neighbours in the helix. Thus, a helix can be modelled as a heterogeneous elastic rod with E and G varying with the type of nearest neighbours. Equilibrium statics says that for a heterogeneous rod composed of N equally spaces subunits, the net torsional constant is:

$$1/C = 1/C_1 + 1/C_2 + \ldots 1/C_n \quad (7)$$

and the bending constant is:

$$1/B = 1/N^2(1/B_1 + 1/B_2 + \ldots 1/B_n) \quad (8)$$

where the subscript n refers to the individual elements of the rod. If, as the data suggest (Fig. 1), DNA stiffness is dominated by the nearest-neighbour interactions and is relatively insensitive to bp inversion we can usefully write the above equations;

$$1/C = \frac{L}{I}(f_{aa}/G_{aa} + f_{ag}/G_{ag} + f_{gg}/G_{gg}) \quad (9)$$

and

$$1/B = \frac{1}{IL}(f_{aa}/E_{aa} + f_{ag}/E_{ag} + f_{gg}/E_{gg}) \quad (10)$$

where L is the overall length of the helix segment in cm, G_{aa} (for example) is the shear modulus between two adjacent A·T bps and f_{aa} is the frequency of AT nearest neighbours, normalized to unity. The value for each element of E or G has been assigned by reference to the consensus values listed in Table 1. Thus, for any DNA segment

$$f_{aa} + f_{ag} + f_{gg} = 1 \quad (11)$$

Using the above formalism, we can evaluate the contribution of DNA stiffness variation to the binding specificity of the 434 repressor. In Table 2 we have catalogued the three base-stacking interactions at the centre of the operator for each of the synthetic binding sites studied by Koudelka *et al.*[2] Based upon those nearest neighbour frequencies, we have used equation (9) to calculate the bending and torsional spring constant for the region (Table 2). Next, as a first approximation, we propose that when DNA sequence is changed at the centre of the operator (where there are no protein contacts), the resulting change in repressor affinity is due exclusively to a change in the binding free energy which must be spent to bend or twist the central DNA segment. This free energy is stored as bending and torsional strain, as described by equations (5) and (6). If two particular operator sequences labelled 1 and 2 have torsional strain energies $U_1(\phi)$ and $U_2(\phi)$ stored for a fixed angular strain ϕ, then the dissociation constant change which results from the stiffness difference can be expressed as the ratio K_1/K_2:

$$K_1/K_2 = \exp[2(U_2(\phi) - U_1(\phi))/kT] \quad (12)$$

Further, by taking the log of both sides of the above equation and substituting in equation (5) we find:

$$\log(\{K_1/K_2\}) = \phi^2/kT \times (C_2 - C_1) \quad (13)$$

Similarly, in terms of bending energetics:

$$\log(K_1/K_2) = 1/kTS^2 \times (B_2 - B_1) \quad (14)$$

Note that in equations (13) and (14) we assume that the twist angle ϕ and the bending radius S each represent one degree of freedom and that the energy of mechanical deformation has a negligible entropy contribution.

The calculated torsion and bending constants are presented for each synthetic operator in Table 2, along with the binding data measured by Koudelka *et al.*[2]. The correlation between theory and experiment is presented in Fig. 2, which shows that the stiffness model accounts well for the sequence dependence of the data. It is interesting that the one sequence permutation which is not adequately fitted by these stiffness calculations is

Table 2 A calculated relation between 434 repressor binding and stiffness

Operator number	Name	Central sequence	f_{aa}	f_{ag}	f_{gg}	C $\times 10^{-12}$	B $\times 10^{-26}$	K_1/K_2 exper	$\log\{K_1/K_2\}$ exper
0	14	ATAT	1	0	0	0.37	1.15	1	0
1	6T	TTAA	1	0	0	0.37	1.15	1.5	0.4
2	6C	CTAG	1/3	2/3	0	0.57	1.8	5	1.6
3	6G	GTAC	1/3	2/3	0	0.57	1.8	5	1.6
4	6G/2	GTAT	2/3	1/3	0	0.45	1.4	2.5	0.9
5	7A	AATT	1	0	0	0.37	1.15	1	0
6	7A/2	AAAT	1	0	0	0.37	1.15	0.3	−1.2
7	7C	ACGT	0	2/3	1/3	0.9	2.8	50	3.9
8	7G	AGCT	0	2/3	1/3	0.9	2.8	50	3.9
9	7G/2	AGAT	1/3	2/3	0	0.57	1.8	7	1.9

The binding data of Koudelka *et al.*[2] have been summarized here. The central DNA sequence of each 14-bp long operator has been specified (positions 6-9). All other nucleotides are unchanged relative to operator 14, which is: ACAATATATATTGT. Binding data (K_1/K_2 experimental) are presented as the repressor dissociation constant, relative to that measured with the unmodified binding site (fragment 14). For example, 50 signifies that in ref. 2, 434 repressor binding to operator 7G was found to be 50 times weaker than to unmodified operator fragment 14. f_{aa}, f_{ag}, f_{gg} refer to the frequency of nearest neighbour associations at the centre of each synthetic operator. C is the calculated torsional spring constant for that central region in units of 10^{-12} dyne, derived by assuming $G_{aa} = 0.167 \times 10^9$ dyne cm^{-2}; $G_{ag} = 0.33 \times 10^9$ dyne cm^{-2}; $G_{gg} = 0.66 \times 10^9$ dyne cm^{-2}. B is the calculated bending constant for the central region, in units of 10^{-26} dyne cm^2, derived by assuming $E_{aa} = 0.5 \times 10^9$ dyne cm^{-2}; $E_{ag} = 1.0 \times 10^9$ dyne cm^{-2}; $E_{gg} = 2.0 \times 10^9$ dyne cm^{-2}. See text for details.

7A/2 (number 6 in Fig. 2). That manipulation creates a three-nucleotide oligo-(A) sequence at the centre of the synthetic operator (Table 2). Such oligo-(A) segments have been described as the source of permanent helix bends[11,14,15]. Our simple elastic analysis has probably failed to account for such a secondary structural effect in operator 6.

Although Anderson *et al.* point out that the centre 4 bp of the 434 repressor complex is substantially bent and overtwisted[1], the absolute change in twist or curvature cannot yet be determined as the structure of the uncomplexed binding site has not been measured. In the absence of this information, it is useful to quantify the relationship between theory and experiment in Fig. 2 in the context of two limiting models. If it is presumed that the sequence dependence of repressor binding in ref. 2 is determined only by torsional stiffness differences, the slope of Fig. 2 specifies that, within the central 4 bp, 32° of twist change will account for all the measured affinity change among the 10 synthetic binding sites. Also, in terms of bending, a 33 Å radius of curvature would account for all the measured binding constant difference (excluding fragment 6).

From the Anderson *et al.* data[1] it is clear that the bend and twist change occurring on binding 434 repressor is about half that specified by the two limiting models. Consequently, when bending and torsional flexibility are both considered, it is likely that the simple stiffness formalism which we have presented can account for the sequence dependence of 434 repressor binding to its operator sequence, both qualitatively and quantitatively.

Additional experimentation is required to understand the rules relating DNA sequence to DNA flexibility, but the data at hand suggest that the sequence dependence of DNA stiffness may be significant whenever a protein (or other ligand) must bend or twist DNA to form its bound complex. Within the limits of the model, the formalism which we have presented can be used to assess the contribution of bending or twisting energetics to this class of site-specific binding interaction.

This work benefited from discussion with Professor Gerry Manning and Professor Robert Hopkins, who has independently developed a similar model for DNA rigidity as a function of bp composition. R.H.A. acknowledges support from the Office of Naval Research, and M.E.H. from the NSF and the National Cancer Institute.

Received 15 June; accepted 3 August 1987.

1. Anderson, J. E., Ptashne, M. & Harrison, S. C. *Nature* **326**, 846-852 (1987).
2. Koudelka, G. B., Harrison, S. B. & Ptashne, M. *Nature* **326**, 886-888 (1987).
3. Peterlin, A. *Nature* **171**, 259-262 (1953).
4. Landau, L. & Lifshitz, E. M. in *Statistical Physics* (Addison-Wesley, Reading, 1958).
5. Barkley, M. D. & Zimm, B. H. *J. chem. Phys.* **70**, 2991-3007 (1979).
6. Millar, D. P., Robbins, R. J. & Zuwail, A. H. *J. chem. Phys.* **76**, 2080-2094 (1982).
7. Hogan, M., LeGrange, J. & Austin, B. *Nature* **304**, 752-754 (1983).
8. Thomas, T. J. & Bloomfield, V. A. *Nucleic Acids Res.* **11**, 1919-1931 (1983).
9. Chen, H. H., Rau, D. C. & Charney, E. *J. biomolec. struct. Dynam.* **2**, 709-719 (1985).
10. Berkoff, B., Hogan, M., LeGrange, J. & Austin, R. *Biopolymers* **25**, 307-316 (1986).
11. Wu, H. M. & Crothers, D. M. *Nature* **308**, 509-513 (1984).
12. Fujimoto, B. S., Shibata, J. H., Schurr, R. L. & Schurr, J. M. *Biopolymers* **24**, 1009-1022 (1985).
13. Fratini, A. V., Kopka, M. L., Drew, H. R. & Dickerson, R. E. *J. biol. Chem.* **257**, 14686-14707 (1982).
14. Ulanovsky, L., Bodner, M., Trifonov, E. N. & Choder, M. *Proc. natn. Acad. Sci. U.S.A.* **83**, 862-866 (1986).
15. Hagermann, P. *Nature* **321**, 449-450 (1986).

Proline isomerism in staphylococcal nuclease characterized by NMR and site-directed mutagenesis

Philip A. Evans*§, Christopher M. Dobson*, Roger A. Kautz†§, Graham Hatfull‡ & Robert O. Fox†

* Inorganic Chemistry Laboratory, University of Oxford, South Parks Road, Oxford OX1 3QR, UK
† Department of Cell Biology, Stanford University Medical School, Stanford, California 94305, USA
‡ Department of Molecular Biophysics and Biochemistry, Yale University, New Haven, Connecticut 06520, USA

Nuclear magnetic resonance (NMR) studies have shown that two distinct folded conformations of staphylococcal nuclease coexist in solution[1] and that these two states can interconvert directly without passing through an unfolded state. These experiments have also revealed that the two forms have very different folding kinetics, although the possibility that one component is an obligatory intermediate for the folding of the other form could be discounted[1]. Here we report NMR data which show that alternative unfolded states are also distinguishable. These observations led us to hypothesize that *cis/trans* isomerism at a single peptide bond between a proline and its preceding residue might be the origin of the conformational multiplicity. Proline 117 was identified as a likely candidate for the site concerned and a mutant protein, in which Pro 117 was replaced by Gly, was constructed in order to test this. Alternative conformations are not observed in the spectrum of this mutant, lending powerful support to this hypothesis.

The existence of alternative folded states of nuclease is

§ Present addresses: Medical Molecular Biology Unit, Middlesex Hospital Medical School, Cleveland Street, London W1P 6DB, UK (P.A.E.) and Department of Molecular Biophysics and Biochemistry, Yale University, New Haven, Connecticut 06520, USA (R.A.K.).